Excitatory neurons of the proprioceptive, interoceptive, and arousal hindbrain networks share a developmental requirement for *Math1*

Matthew F. Rose[a], Kaashif A. Ahmad[b], Christina Thaller[c], and Huda Y. Zoghbi[a,b,d,e,1]

[a]Program in Developmental Biology, Departments of [b]Pediatrics, [c]Biochemistry and Molecular Biology, and [d]Molecular and Human Genetics, and [e]Howard Hughes Medical Institute, Baylor College of Medicine, Houston, TX 77030

Contributed by Huda Y. Zoghbi, October 7, 2009 (sent for review September 3, 2009)

Hindbrain networks important for sensation and arousal contain diverse neuronal populations with distinct projections, yet share specific characteristics such as neurotransmitter expression. The relationship between the function of these neurons, their developmental origin, and the timing of their migration remains unclear. Mice lacking the proneural transcription factor *Math1* (*Atoh1*) lose neurons essential for hearing, balance, and unconscious proprioception. By using a new, inducible *Math1*^{Cre*PR} allele, we found that *Math1* is also required for the conscious proprioceptive system, including excitatory projection neurons of the dorsal column nuclei and for vital components of the interoceptive system, such as Barrington's nucleus, that is closely associated with arousal. In addition to specific networks, *Math1* lineages shared specific neurotransmitter expression, including glutamate, acetylcholine, somatostatin, corticotropin releasing hormone, and nitric oxide. These findings identify twenty novel *Math1* lineages and indicate that the *Math1* network functions partly as an interface for conscious (early-born) and unconscious (late-born) proprioceptive inputs to the cortex and cerebellum, respectively. In addition, these data provide previously unsuspected genetic and developmental links between proprioception, interoception, hearing, and arousal.

auditory | dorsal columns | medial lemniscus | proneural | rhombic lip

Movement requires an accurate representation of body position in space that utilizes multiple sensory inputs to the hindbrain, including the auditory, vestibular, and proprioceptive systems. It also requires regulation of an organism's arousal state, which sensory systems modulate by stimulating the hindbrain nuclei of the reticular activating system.

Interestingly, many components of these various systems share a developmental requirement for the proneural transcription factor *mouse atonal homolog 1* (*Math1*, *Atoh1*) (1–6). *Math1* expression begins around embryonic day E9.5 in the rhombic lip (RL), the dorsal-most neuroepithelium of the developing hindbrain, and spans the length of the pons, cerebellum, and medulla (7, 8). Early *Math1*-dependent neuronal populations have been identified primarily in the rostral pons and cerebellum by using *Math1 lacZ* knock-in and *Math1-creERT2* transgenic mice (1, 3, 4), whereas the caudal pons and medulla have remained comparatively uncharacterized due to technical constraints, leaving open the possibility that the full extent of *Math1*'s contribution to various hindbrain networks has yet to be revealed.

Proprioception has been divided anatomically into unconscious and conscious pathways. In the unconscious pathway, sensory inputs synapse with precerebellar neurons in the spinal cord and in the external cuneate nucleus (ECu) in the medulla, and then project to the cerebellum to coordinate movement "unconsciously" (9). The conscious proprioceptive network, by contrast, sends input to the cortex via the cuneate and gracile dorsal column nuclei in the medulla (10), which relay it to the thalamus via excitatory glutamatergic fibers in the medial lemniscus (11). *Math1* is required for glutamatergic neurons in the ECu and other precerebellar nuclei (unconscious proprioception), but no reports have linked *Math1* with conscious proprioception. Indeed, the origin of the dorsal column nuclei as well as their genetic relationship to ECu neurons has remained unclear.

Similarly, auditory information projects along two distinct hindbrain pathways, from the ventral cochlear nucleus (VC) to either the adjacent dorsal cochlear nucleus (DC) or the superior olive nucleus (SON) in the ventral medulla. The DC analyzes frequency differences whereas the SON determines the source of sounds relative to the position of the body (12, 13). Both pathways send excitatory glutamatergic projections via the lateral lemniscus to the inferior colliculus (12, 14, 15). However, although RL-derived glutamatergic neurons of the VC and DC require *Math1* (3, 16), the origin of the SON has yet to be reported.

In this study, we generated a targeted hormone-inducible *Math1*^{Cre*PR} allele to ensure a native *Math1* expression pattern. We labeled temporally distinct subsets of *Math1*-expressing lineages and traced their projections. In addition, we characterized changes in neurotransmitter expression in the perinatal hindbrain of *Math1*-null mice. These experiments revealed a novel *Math1*-dependent caudal RL migratory stream in the medulla, doubled the number of reported *Math1* hindbrain lineages, and identified new *Math1*-dependent neurotransmitters of the conscious proprioceptive, interoceptive ("visceral proprioceptive"), vestibular, auditory, and arousal networks.

Results

Novel *Math1* Lineages in the Medulla and Pons. Known *Math1*-dependent caudal rhombic lip (cRL) lineages migrate in the posterior precerebellar extramural migratory stream (PES) over several days to form the ECu and lateral reticular (LRt) nuclei in the medulla (3, 6, 17). The peak migration occurs around E12 in mice (18). By using *Math1*$^{LacZ/+}$ knock-in mice (1), we uncovered an earlier migration from the cRL at E10.5 (Fig. 1*A*, yellow arrow) that was contiguous with the later-forming PES (black arrowhead). This early migration, which we term the caudal rhombic-lip migratory stream (CLS), appeared to form several unreported *Math1* lineages in the medulla (Fig. 1*A*, yellow arrowheads). Serial coronal sections through an E16.5 *Math1*$^{LacZ/+}$ hindbrain identified many nuclei containing new *Math1* lineages in both the medulla and caudal pons (Fig. S1), summarized in Fig. 1*B′* (dark blue) in relation to known lineages (light blue), as best approximated from multiple brain atlases (*SI Text*).

Temporal Classification of *Math1* Hindbrain Lineages. To better assess the fate of these new *Math1* lineages and characterize the time of their formation, we targeted a hormone-inducible *Cre*PR* con-

Author contributions: M.F.R. and H.Y.Z. designed research; M.F.R., K.A.A., and C.T. performed research; M.F.R. analyzed data; and M.F.R., K.A.A., and H.Y.Z. wrote the paper.

The authors declare no conflict of interest.

[1]To whom correspondence should be addressed. E-mail: hzoghbi@bcm.tmc.edu.

This article contains supporting information online at www.pnas.org/cgi/content/full/0911579106/DCSupplemental.

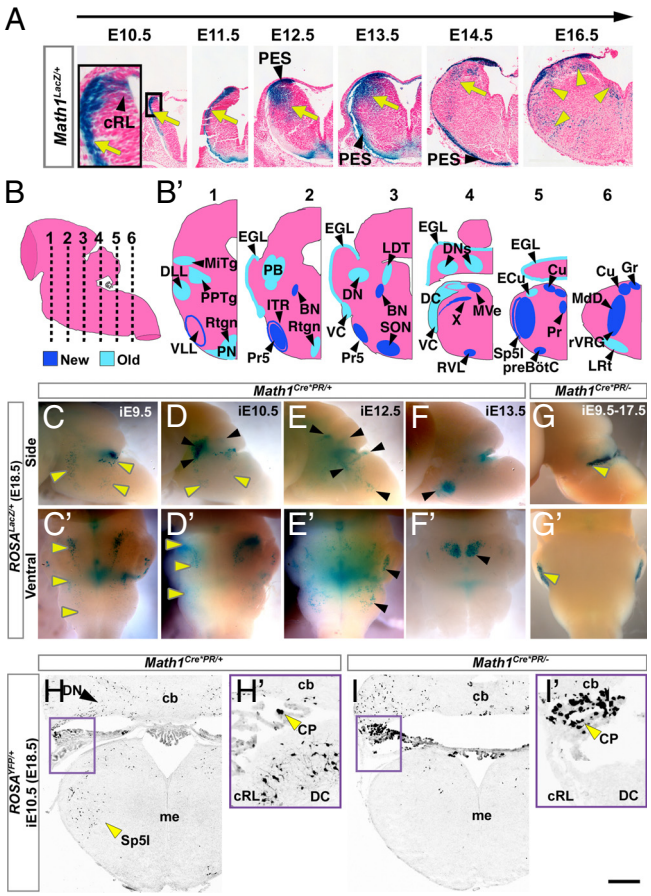

Fig. 1. Novel early-forming *Math1* lineages in the medulla and caudal pons. (*A*) Time course (E10.5–16.5) of LacZ expression in the medulla of $Math1^{LacZ/+}$ mice (approximately level 5 in *B′*). An early migration (yellow arrows) from the cRL is seen several days before the PES (black arrowheads), giving rise to novel *Math1* lineages (yellow arrowheads). (*Inset*) cRL and migrating cells (yellow arrow) at E10.5. (*B*) Brainstem schematic. Lines 1–6 indicate coronal hemisection levels shown in (*B′*) depicting nuclei that contain new (dark blue) and known (light blue) *Math1* lineages. (*C–F*) Side views of whole-mount E18.5 $Math1^{Cre*PR/+}$;$ROSA^{LacZ/+}$ hindbrains induced on E9.5, E10.5, E12.5, or E13.5, showing LacZ-labeled cell somas (blue) of new (yellow arrowheads) and known (black arrowheads) lineages. (*G*) A $Math1^{Cre*PR/-}$;$ROSA^{LacZ/+}$ (*Math1*-null) hindbrain induced daily (E9.5 to E17.5) had staining mainly at the cRL (yellow arrowhead). (Some background fourth-ventricle staining was visible due to tissue clearing). (*C′–G′*) Ventral surfaces of *C–G*. (*H* and *I*) Coronal sections from E18.5 $Math1^{Cre*PR/+}$; $ROSA^{EYFP/+}$ (*H*) and $Math1^{Cre*PR/-}$; $ROSA^{EYFP/+}$ (*I*) null hindbrains induced at E10.5, showing loss of most staining from the medulla in the *Math1*-null. (*H′* and *I′*) Magnified boxed regions in *H* and *I*, from slightly more rostral positions, show primarily labeled DC neurons in $Math1^{Cre*PR/+}$ and CP cells in $Math1^{Cre*PR/-}$ (yellow arrowhead), adjacent to the cRL. Lateral to left in *A* and *B′* and *H–I′*; rostral to left in *B* and *C–G*; rostral up in *C′–G′*. Abbreviations: cRL, caudal rhombic lip; CP, choroid plexus. See Table 1 for other abbreviations. (Scale bar: *A*, 290 μm; *A Inset*, 60 μm; *C–G*, 1,000 μm; *C′–G′*, 900 μm; *H* and *I*, 400 μm; *H′* and *I′*, 100 μm.)

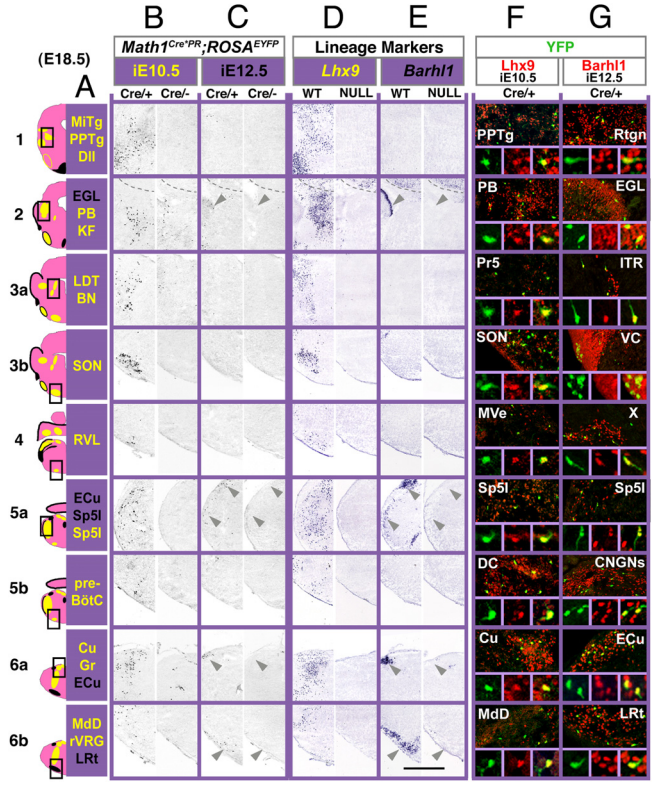

Fig. 2. Temporally similar *Math1*-dependent neurons share marker expression. (*A*) Schematics of hindbrain nuclei containing early- (yellow) and late-forming (black) *Math1* lineages (listed to right in corresponding colors) on coronal hemisections, rostral to caudal (levels 1–6, Fig. 1*B*). (*B* and *C*) Magnified boxed regions in *A* from corresponding sections of E18.5 $Math1^{Cre*PR/+}$;$ROSA^{EYFP/+}$ and $Math1^{Cre*PR/-}$;$ROSA^{EYFP/+}$ null mice induced at E10.5 (*B*) or E12.5 (*C*). (Dashed line at level 2 marks the midbrain/hindbrain junction.) The regions shown contain mainly E10.5 populations, so E12.5 populations are marked by gray arrowheads. (*D* and *E*) Corresponding regions to *B* and *C* from E18.5 WT and *Math1*-null hindbrains were stained either with *Lhx9* (*D*) or *Barhl1* (*E*) (gray arrowheads) ISH probes. Most *Lhx9* and *Barhl1* expression was lost in *Math1*-null hindbrains, whereas some expression persisted in non-*Math1* lineages of the midbrain. (*F* and *G*) Colabeling of anti-GFP (green) with anti-Lhx9/Lhx2 (red) or anti-Barhl1 (red) when induced at E10.5 (*F*) or E12.5 (*G*), respectively, in select $Math1^{Cre*PR/+}$;$ROSA^{EYFP/+}$ hindbrain nuclei. These regions, labeled by nucleus, do not correspond to the boxes in *A*. Higher magnifications below each region show that Lhx9 is expressed in early-born neurons and Barhl1 is expressed in later-born neurons. Abbreviations: Please see Table 1 for list of nuclei. (Scale bar: *B–E*, 500 μm; *F* and *G*, 83 μm; *F* and *G Insets*, 28 μm.)

struct into the *Math1* locus (Fig. S2). We crossed $Math1^{Cre*PR/+}$ mice to $ROSA^{LacZ/+}$ Cre reporter mice (19) and induced Cre activity with single doses of RU486 on E9.5, E10.5, E12.5, or E13.5. Analysis at E18.5 revealed distinct and reproducible patterns of labeled hindbrain cells for each induction time, indicating a temporal resolution of at least 24 h for this Cre. The labeling included new (yellow arrowheads) and known (black arrowheads) *Math1* lineages (Fig. 1*C–F′*), and persisted in the adult (Fig. S3). In contrast, Cre induction in mice lacking *Math1* ($Math1^{Cre*PR/-}$;$ROSA^{LacZ/+}$) primarily labeled cells near the RL (Fig. 1 *G* and *G′*). For higher resolution imaging, we crossed $Math1^{Cre*PR}$ mice to the $ROSA^{EYFP}$ Cre-reporter line (20). *Math1*-null brains (E18.5) induced at E10.5 had increased labeling of the choroid plexus (CP), with a concordant decrease in *Math1* medullary lineages (compare Fig. 1 *I* and *H*). Because the CP arises from the roof plate, immediately adjacent to the RL (21), this observation parallels that in the spinal cord where *Math1*-dependent lineages contribute to the roof plate in *Math1*-null mice (22).

The schematics in Fig. 2*A* summarize nuclei containing *Math1* populations labeled at E10.5 (yellow) versus E12.5/E14.5 (black), with boxed regions shown to the right (Fig. 2 *B* and *C*). The conscious proprioceptive nuclei were labeled primarily at E10.5 and included the cuneate (Cu) and gracilis (Gr) dorsal column nuclei (Fig. 2*B*, level 6a), and the principal sensory trigeminal (Pr5) and medial portion of the spinal trigeminal–interpolar division (Sp5I) nuclei (Fig. 2*B*, level 5a, 2*F*). In contrast, most unconscious proprioceptive lineages were labeled at E12.5–E14.5, including the external granule layer (EGL), ECu, and LRt (Fig. 2*C*, levels 2, 6a, 6b), as well as the lateral portion of Sp5I (Fig. 2*C*, level 5a), and the intertrigeminal region (ITR), prepositus (Pr), and roller precer-

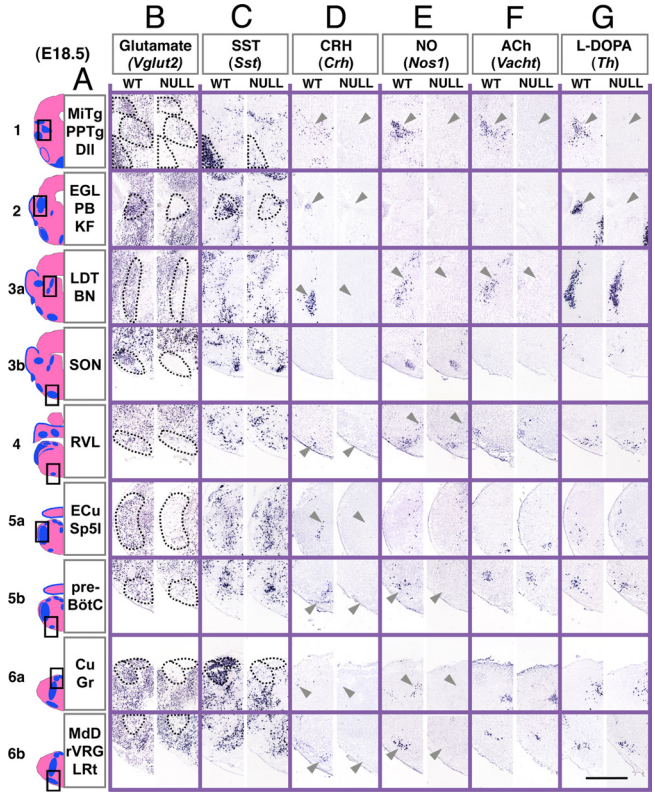

Fig. 3. Subsets of glutamatergic, somatostatin, CRH, nitric oxide, cholinergic, and L-dopa neurons require *Math1*. (*A*) Schematics of hindbrain nuclei containing *Math1* lineages (blue, listed to right) on coronal hemisections, rostral to caudal (levels 1–6, Fig. 1*B*). (*B–G*) Magnified boxed regions in *A* from corresponding E18.5 WT and *Math1*-null sections stained with ISH probes for glutamate (*Vglut2*), somatostatin (SST: *Sst*), corticotropin releasing hormone (CRH: *Crh*), nitric oxide (NO: *Nos1*), acetylcholine (ACh: *Vacht*), and levodopa (L-Dopa: *tyrosine hydroxylase*, *Th*) neurons. Nuclei containing *Math1*-dependent *Vglut2* or *Sst* are marked by dotted outlines, whereas other *Math1*-dependent neurotransmitters are marked by gray arrowheads. Abbreviations: Please see Table 1 for list of nuclei. (Scale bar: *B–G*, 500 μm.)

ebellar nuclei (Fig. 2*G*). Similarly, neurons of the medial (MVe) and spinal (SpVe) vestibular nuclei were labeled at E10.5 (Fig. 2*F*), whereas the more lateral vestibular nucleus X (X) was labeled at E12.5 (Fig. 2*G*). In the auditory system, central neurons of the SON and DC were labeled at E10.5 (Fig. 2*B*, level 3b, and 2*F*), whereas the more lateral VC and cochlear granule neurons were labeled at E12.5 (Fig. 2*G*).

Induction at E10.5 also labeled nuclei vital for interoception, including Barrington's (BN) and the parabrachial/Kölliker-Fuse (PB/KF) nuclei (Fig. 2*B*, levels 2, 3a), as well as those critical for arousal: the pedunculopontine tegmental (PPTg), lateral dorsal tegmental (LDT), and medullary reticular (MdD) nuclei (Fig. 2*B*, levels 1, 3a, 6b). Moreover, induction at E10.5 labeled cells near multiple medullary nuclei associated with respiration: the rostroventrolateral reticular nucleus (RVL), pre-Bötzinger complex (preBötC), and rostral ventral respiratory group (rVRG) (Fig. 2*B*, levels 4, 5b, 6b), recently described in further detail (23). Table 1 lists all new and known *Math1* hindbrain populations.

We also evaluated several transcription factors and neurotransmitter markers to help control for confounding factors, such as *Math1* autoregulation (24). Expression of *Lhx9* and *Barhl1* at E18.5, known *Math1*-dependent transcription factors (3, 6, 25), segregated with *Math1* lineages induced at E10.5 and E12.5, respectively (Fig. 2 *D–G*), and were lost in *Math1*-null hindbrains (Fig. 2 *D* and *E*). *Lhx2* and *Barhl2*, also *Math1*-dependent (6, 26),

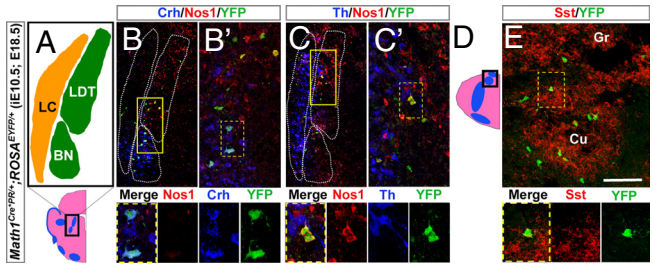

Fig. 4. Nitric oxide, CRH, and somatostatin neurons of the arousal, interoceptive, and conscious proprioceptive systems arise from the RL. (*A*) Schematic of coronal hemisection with nuclei containing *Math1* lineages (blue); boxed region magnified above shows the LDT and BN (green) medial to the LC (orange). (*B* and *C*) Dotted outlines mark approximate boundaries of these three nuclei on adjacent sections from a $Math1^{Cre*PR/+}$;$ROSA^{EYFP/+}$ hindbrain (E18.5) induced at E10.5 and stained for EYFP (green) and Nos1 (red) with either Crh (*B*) (blue) or Th (*C*) (blue). (*B′* and *C′*) Regions magnified from yellow boxes in *A* and *B* with yellow dashed boxes further magnified below each. EYFP colabeled with Crh and Nos1 but not with Th. (*D*) Schematic showing nuclei containing *Math1* lineages (blue) on a coronal hemisection from the caudal medulla. (*E*) Boxed region from *D* shows EYFP and Sst expression in the Cu/Gr nuclei. Dashed box, magnified below, shows colabeling of EYFP (somas) with Sst (cytoplasmic + extracellular). Abbreviations: CRH, corticotropin releasing hormone; Nos1, nitric oxide synthase 1; Sst, somatostatin. See Table 1 for other abbreviations. (Scale bar: *B* and *C*, 250 μm; *B′*, *C′*, and *E′*, 80 μm; *Lower* frames of *B*, *C*, and *E*, 40 μm.)

appeared similar to *Lhx9* [Movies S1–S48 (AVI)]. [These lineages did not coexpress Phox2b, distinguishing them from recently identified neurons with intraparenchymal *Math1* expression (23).] Complete sets of serial sections labeled for each transcription factor in both WT and *Math1*-null hindbrains are available online [Movies S1–S48 (AVI)].

Subsets of Hindbrain Glutamatergic, Somatostatin, CRH, Nitric Oxide, Cholinergic, and Levodopa Neurons Require Math1. Loss of *Math1* led to loss/reduction in markers for multiple hindbrain neurotransmitters: glutamate (*Vglut1*, *Vglut2*, and *Vglut3*), somatostatin (*Sst*), corticotropin releasing hormone (*Crh*), nitric oxide (*Nos1*), acetylcholine (*Vacht*), and levodopa (*Th*) [Fig. 3 *B–G*, Table 1, and Movies S1–S48 (AVI)]. *Vglut2* was largely absent from the *Math1*-null dorsal lateral lemniscal (Dll), lateral PB, and SON nuclei in the pons (Fig. 3*B*, levels 1, 2, 3b), and the Cu/Gr dorsal column nuclei in the medulla (Fig. 3*B*, level 6a). Other nuclei primarily lost neurons with high *Vglut2* expression, whereas low-expressing ones remained, presumably from non-*Math1*-dependent lineages (27): the microcellular tegmental (MiTg), PPTg, LDT/BN, Sp5I, RVL, MdD, rVRG, and near the preBötC (Fig. 3*B*, levels 1, 3a, 4, 5a, 5b, 6b). Several other regions likewise lost many *Vglut2 neurons* [Movies S1–S48 (AVI), Table 1]. We quantified the *Vglut2* expression change in each region pictured (Fig. S4). *Vglut1*, expressed primarily by the VC at P0, was entirely lost. Most other neurons that express *Vglut1* later (e.g., granule and precerebellar neurons) also require *Math1* (1–3). By comparison, *Vglut3* was only lost from the DC [Movies S1–S48 (AVI)]. The Dll and PB in the pons and the Cu/Gr in the medulla also lost much of their *Sst* expression (Fig. 3*C*, levels 1, 2, 6a).

Math1-null mice also lost most *Crh* expression from the hindbrain, including the PPTg, PB, and BN in the pons, and the RVL, Sp5I, ECu, preBötC, Cu, and LRt in the medulla (Fig. 3*D*, levels 1–3a, 4–6b). *Nos1* was similarly lost from the PPTg and LDT of the pons, components of the reticular activating system (Fig. 3 *E* and *F*, levels 1, 3a), and from the preBötC, Cu, and rVRG in the medulla (Fig. 3 *E* and *F*, levels 5b–6b). *Vacht* was likewise lost from the PPTg and LDT, indicating these cholinergic neurons require *Math1* in addition to being *Math1*-derived (4). Interestingly, the PPTg and PB also expressed *Math1*-dependent tyrosine hydroxylase (*Th*) (Fig. 3*G*, levels 1–2) but lacked subsequent enzymes required for nor-

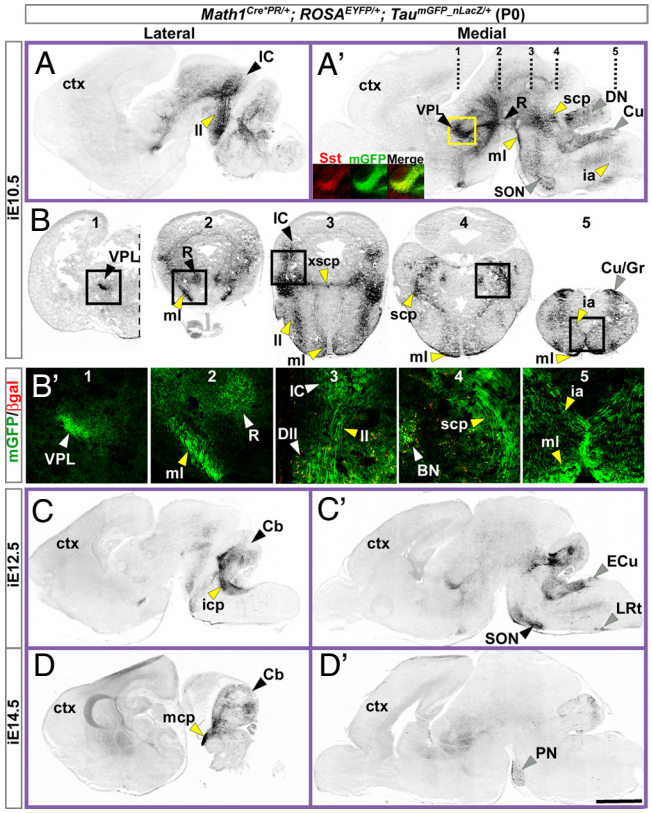

Fig. 5. Early *Math1* lineages project in the medial and lateral lemnisci and the superior cerebellar peduncle. *Math1*$^{Cre*PR/+}$; *ROSA*$^{EYFP/+}$; *Tau*$^{mGFP\_nLacZ/+}$ hindbrains (P0) induced at E10.5 (*A*–*B*′), E12.5 (*C*), or E14.5 (*D*). (*A* and *A*′) Lateral (*A*) and medial (*A*′) sagittal sections showing mGFP-labeled projections (black) with indicated sources (gray arrowheads) and known targets (black arrowheads) of selected projections (yellow arrowheads), including those in the ll, ml, and scp. *Insets* (from yellow box) show overlapping expression of mGFP and Sst processes in the VPL thalamic nucleus. (Although somas also expressed EYFP, primarily mGFP processes were visible at this magnification.) (*B*) Coronal sections from positions 1–5 (dotted lines on *A*′). Section level 1 is a hemisection (dashed line). (*B*′) Magnified boxed regions from *B* show mGFP processes (green) and βgal-labeled somas (red) (from the *Tau*$^{mGFP\_nLacZ/+}$), with selected projections (yellow arrowheads) and nuclei (white arrowheads) indicated. (*C*–*D*′) Lateral (*C* and *D*) and medial (*C*′ and *D*′) sagittal sections showing projections in the icp (*C*) and mcp (*D*) when induced at E12.5 and E14.5, respectively. Abbreviations: Sst, somatostatin; R, red nuclei; VPL, ventral posterolateral nuclei; IC, inferior colliculus; ctx, cortex; ia, internal arcuate fibers; ml, medial lemnesci; ll, lateral lemnesci; scp, superior cerbellar peduncles; icp, inferior cerebellar peduncles; mcp, middle cerebellar peduncles. See Table 1 for other abbreviations. (Scale bar: *A*, *A*′, and *C*–*D*′, 1,100 μm; *B*, 800 μm; *B*′, 215 μm.)

Table 1. Summary of the *Math1* hindbrain rhombic lip lineages

Nuclei (abbre)	Nuclei containing *Math1*-dependent neurons	Migration stream	Time: E15.5-P0	Time: E12.5-14.5	Time: E11.5-12.5	Time: E9.5-10.5	Neurotransmitters: *Vglut1*	*Vglut2*	*SST*	*Penk1*	*CRH*	*NOS1*	*Vacht*	*TH*	*Vglut3*	TFs: *Barh1*	*Barh2*	*Lhx9*	*Lhx2*	Function: P-uncon	P-cons	Hearing	Interocep	Arousal	Breathing	Ref
Cerebellum & Rostral Pons																										
Cerebellum																										
UPBCs	unipolar brush cells	RLS	+				+	+												+						6
CbGNs	cb granule progenitors	RLS (EGL)	+	+			+									+				+						1
DN(F)	fastigial deep cerebellar	RLS (NTZ)			+	+		+		+						+				+						4,5
DN(D)	dentate deep cerebellar	RLS (NTZ)				+		+										+		+						4,5
PBG	parabigeminal	RLS			+			+										+						+		4,5
MiTg	microcellular tegmental	RLS			+	+		+										+						+		4,5
DLL	dorsal lateral lemniscal	RLS				+		+	+								+	+	+			+				4,5
KF	Kölliker-Fuse	RLS				+		+									+						+		+	7
MPL	medial paralemniscal	RLS				+		+									+	+	+			+				●
MPB	medial parabrachial	RLS				+		+										+						+		●
PnO	pontine reticular-oral part	RLS				+					+							+						+		●
LPB	lateral parabrachial	RLS			+	+		+	+	+	+				+			+	+	+			+		+	4,5
PPTg	pedunculopontine teg.	RLS				+		+			+	+	+	+				+						+		4,5
Caudal Pons																										
PN	pontine	AES		+			+		+							+				+						2
Rtgn	reticulotegmental	AES		+			+		+							+				+						4,5
ITR	intertrigeminal region	AES			+		+									+		+		+					+	●
Pr5	prin. sensory trigeminal					+		+										+			+					●
SON	superior olive					+		+										+	+			+				●
BN	Barrington's					+					+												+	+		●
LDT	lateral dorsal tegmental					+							+	+				+							+	5
SuVe	superior vestibular					+		+									+		+	+			+			4
Rostral Medulla																										
Cochlear Nucleus																										
CNGNs	cochlear granule cells	CES		+			+									+						+				4
VC	ventral cochlear	CES			+		+	+	+										+			+				4
DC	dorsal cochlear	CES				+		+				+			+			+	+			+				4
X	nucleus X (vestibular)				+		+									+				+			+			●
SpVe	spinal vestibular					+		+									+	+		+			+			●
MVe	medial vestibular					+		+										+		+			+			●
Pr	prepositus				+		+				+					+				+						●
Ro	roller				+		+				+					+				+						●
RVL	rostroventrolateral retic.	CLS				+		+			+	+						+	+					+		●
Caudal Medulla																										
ECu	external cuneate	CLS (PES)			+		+				+					+				+						3
LRt	lateral reticular	CLS (PES)			+		+				+					+				+						4
Sp5I	spinal trigem. interpolar																									●
Lat	Sp5I-lateral part	CLS (PES)				+		+								+										●
Med	Sp5I-medial part	CLS				+		+				+					+	+	+		+					●
Gr	gracilis	CLS				+		+	+								+	+	+		+					●
Cu	cuneate	CLS				+		+	+			+					+	+	+		+					●
MdD	medullary reticular-dorsal	CLS				+		+									+	+	+					+		●
preBötC	pre-Bötzinger complex	CLS				+		+			+	+						+	+						+	●
rVRG	rostral ventral resp. group	CLS				+		+				+						+	+						+	●

Abbreviations: neurotransmitter markers (Neurotransmitters) transcription factors (TFs), unconscious proprioception (P-uncon), conscious proprioception (P-cons), interoception (Interocep), nuclear transitory zone (NTZ), and the anterior precerebellar extramural (AES), caudal rhombic lip (CLS), cochlear extramural (CES), rostral rhombic lip (RLS), and posterior precerebellar extramural (PES) migratory streams

\+ Indicates approximate formation time, neurotransmitter markers eventually expressed, known *Math1*-dependent transcription factors expressed at E18.5, and the purported function for each *Math1* lineage

Ref # Known *Math1* lineages: (1) Ben-Arie et al., 1997; (2) Ben-Arie et al., 2000; (3) Bermingham et al., 2001; (4) Wang et al., 2005; (5) Machold and Fishell, 2005; (6) Englund et., 2006; (7) Gray et al., 2008

● New *Math1* lineages

epinephrine/dopamine synthesis [Fig. S5 and Movies S1–S48 (AVI)]. These neurons may produce levodopa, similar to more rostral neurons that are reportedly involved in interneuronal shuttling for catecholamine production (28). Also, some enkephalin (*Penk1*) expression was lost from the PB and DN, *serotonin receptor 1a* (*Htr1a*) disappeared from the Dll, and *somatostatin receptor 2* (*Sstr2*) was lost from the EGL and DC [Movies S1–S48 (AVI)]. In contrast, other neurotransmitter markers for GABA, glycine, norepinephrine, dopamine, serotonin, substance P, and thyrotropin releasing hormone showed only slight rearrangements due to loss of surrounding *Math1* lineages [Fig. S5 and Movies S1–S48 (AVI)].

To assess the cell autonomy of these new *Math1*-dependent neurotransmitters, we evaluated the coexpression of EYFP with Nos1, CRH, and SST in select nuclei from *Math1*$^{Cre*PR/+}$;*ROSA*$^{EYFP/+}$ hindbrains induced at E10.5. We found colabeling of early *Math1* lineages with Nos1 in the LDT and CRH in the adjacent BN in the pons (Fig. 4 *A*--*C*), and with SST in the Cu/Gr dorsal column nuclei in the medulla (Fig. 4 *D* and *E*).

***Math1* Lineages Form the Excitatory Hindbrain Output Tracts for Conscious and Unconscious Proprioception and Hearing.** The primary excitatory output tracks for the conscious and unconscious proprioceptive and auditory systems are formed by glutamatergic neurons within the Cu/Gr, DN, and DC/SON, respectively (9, 11, 12). To assess whether the *Math1* lineages in these nuclei correspond to these excitatory projection neurons, we labeled their processes with membrane-targeted GFP by crossing the *Math1*^{Cre*PR} to *Tau*$^{mGFP\_NLacZ}$ Cre-reporter mice (29).

Induction at E10.5 labeled decussating internal arcuate fibers (ia) from the Cu/Gr nuclei to the medial lemniscus (ml) in the ventral medulla (Fig. 5*A*′, and Fig. 5 *B and B*′, level 5). The ml was labeled along its entire length (Fig. 5*B*, levels 2–5) up to the VPL nucleus of the thalamus (Fig. 5 *A*′ and *B*′, level 1), where the labeled fibers overlapped with somatostatin (Sst) expression (Fig. 5*A*′ *Inset*). This thalamic Sst expression is known to arise from the cuneothalamic projections of the dorsal column nuclei, which coexpress Sst and Vglut2 (11). Induction at E10.5 also labeled the lateral lemniscus (ll) that contains axons of the auditory system from the SON and DLL to the inferior colliculi (Fig. 5 *A* and *B*′, level 3). Likewise, projections of the deep cerebellar nuclei extended through the superior cerebellar peduncle (scp) (Fig. 5 *A*′ and *B*′, level 4) and decussated in the pons (xscp) (Fig. 5*B*, level 3) to contralateral red nuclei (R), key targets of the cerebellar nuclei (Fig. 5 *A*′ and *B*′, level 2).

In contrast, induction at E12.5 labeled fibers of the inferior

cerebellar peduncle (Fig. 5*C*) through which the ECu and LRt project (Fig. 5*C′*), and induction at E14.5 labeled fibers of the middle cerebellar peduncle (Fig. 5*D*) known to contain the PN projections (Fig. 5*D′*). Likewise, projections to the SON (likely from the VC) were seen with induction at E12.5 (Fig. 5*C′*).

Discussion

In this study, we combined histological analysis, in situ hybridization, and fate-mapping to identify unreported *Math1*-dependent lineages in the perinatal hindbrain. We find that throughout the hindbrain, distinct subsets of *Math1*-dependent rhombic lip (RL) lineages express the same transcription factors and neurotransmitters and contribute to nuclei of the same networks. Within the conscious and unconscious proprioceptive, interoceptive, auditory, and arousal networks, *Math1* lineages appear to serve similar functions, such as forming the primary excitatory output tracts. It is remarkable that distinct hindbrain networks which process divergent types of sensory information, all rely on the contribution of *Math1*-dependent rhombic lip lineages.

The hindbrain is arranged as a series of anterior–posterior segments or rhombomeres, each of which contains similar neuronal subtypes dependent on many of the same genes (3, 30–32). We find that similar *Math1*-dependent lineages arise from the RL at comparable times in various rhombomeres. The early migration (E9.5–10.5) of the CLS of the medulla occurs in parallel to the early portion of the rostral RL migratory stream (RLS) that populates the cerebellum and pons (3). Both of these early migrations generate *Vglut2*-positive neurons and express *Lhx9*. In contrast, the external granule layer and posterior precerebellar extramural migratory stream (PES), which exit the RL at E12.5–14.5 as later portions of the RLS and CLS, respectively (3, 17), form *Vglut1*-positive neurons that express *Barhl1*. Thus, distinct *Math1* lineages arising in the RL at similar times in different rhombomeres share parallel developmental trajectories and gene expression.

Proprioception, originally defined as an organism's awareness of its own movement and position of its body parts, includes both a conscious network that transmits sensory information to the cortex (10) and an unconscious cerebellar network that coordinates locomotion (9, 33). Although many glutamatergic neurons of the unconscious network, including the ECu in the dorsal medulla, are known to arise from the RL and require *Math1* (1–6, 17), little is known about the origins of conscious proprioceptive neurons. The Cu/Gr dorsal column nuclei, essential for conscious proprioception, lie adjacent to the ECu (10). The majority of Cu/Gr neurons form two days before the ECu (18, 34), and many express *Vglut2* and *Sst* and project to the thalamus via well-defined tracks, including the medial lemniscus (11). We show that the Cu/Gr contain *Math1* lineages arising mostly at E10.5, matching the peak time of formation for Cu/Gr neurons (18), and express Lhx9 and Sst. In addition, they project via the medial lemniscus to the thalamus where their projections overlap with Sst processes. In the absence of *Math1*, the Cu/Gr nuclei lose most all *Vglut2* and *Sst* expression. Hence, the excitatory neurons of conscious and unconscious proprioception in the medulla appear to arise from the RL as early and late portions of the CLS migration, respectively. Their positional, functional, and gene-expression differences correspond to this temporal distinction, with *Math1* serving a central role in the development of both proprioceptive pathways.

This developmental pattern parallels that in the vestibular and auditory systems, where we now show that *Lhx9*-expressing glutamatergic projection neurons of the SON arise early from the RL and require *Math1* just like those of the dorsal cochlear nucleus. Thus, we find that many glutamatergic neurons of the auditory, vestibular, and proprioceptive systems throughout the hindbrain require *Math1*, arise from the rhombic lip at similar times, share expression of specific neurotransmitters and transcription factors, and appear to serve similar roles in each system.

Many NO and CRH neurons critical for interoception and arousal also require *Math1*. The *Math1*-dependent NO lineages include those in the pedunculopontine tegmental (PPTg) and lateral dorasal tegmental (LDT) nuclei in the pons. Together with the adjacent norepinephrine (NE) neurons of the locus coeruleus (LC, A6), these NO neurons, which coexpress acetylcholine (4, 35), constitute an important component of the reticular activating system (RAS) vital for arousal. Likewise, CRH neurons in the PPTg and in Barrington's nucleus (BN), located immediately adjacent to the LDT and LC (36), are also *Math1*-dependent. The BN contains the largest group of CRH neurons in the hindbrain, responds to the interoceptive inputs of bladder and colon distension, and projects to the LC to increase the activity of NE neurons and stimulate arousal (37–39).

This LDT/BN/LC complex lies at a functional intersection of arousal and interoception. Although these three nuclei have been described as anatomically separate, in some species their respective NO, CRH, and NE neurons are intermingled (40). This pattern of associated NO, CRH, and catecholaminergic neurons repeats throughout the hindbrain, including the PPTg and more caudal A5, A1/C1, and A2/C2 nuclei. Although the NE neurons in each of these regions require the proneural gene *Mash1* (31), we now demonstrate that the associated NO and CRH neurons in each case share a similar dependence on *Math1*. These results uncover a previously unsuspected genetic and developmental relationship between CRH and NO neurons of the interoceptive and arousal systems, and suggests a model of these neurons forming together throughout the hindbrain similar to the proprioceptive system.

Many of the *Math1* hindbrain lineages are known to connect with each other within specific networks. In addition, some *Math1*-dependent neurons form connections between the networks. For instance, the PPTg neurons of the RAS receive extensive auditory inputs that have been proposed to mediate the auditory startle response that provides arousal from sleep (41). Similarly, the CRH neurons of the BN connect with the RAS to stimulate arousal in response to interoceptive input (38, 39). The NO/acetylcholine neurons of the RAS connect back to proprioceptive nuclei such as the spinal trigeminal nucleus in the medulla, where cholinergic stimulation increases the excitability of glutamatergic projection neurons (42). Some of these neurons then connect to the thalamus as part of conscious proprioception and others contribute to the cerebellar unconscious proprioceptive network (34). This association between developmental origin and subsequent functional connectivity forms a leitmotif throughout *Math1*-dependent hindbrain networks.

In summary, the present study has doubled the number of known *Math1*-dependent hindbrain lineages and demonstrated that differences in marker expression correlate with temporal origin. Patterns of RL lineage development are conserved throughout the hindbrain, including the differentiation of specific neurotransmitter fates (glutamate, somatostatin, CRH, nitric oxide, acetylcholine, and levodopa). This study provides evidence for the association between *Math1* and conscious proprioception and identifies new *Math1*-dependent components of the unconscious proprioceptive, auditory, vestibular, interoceptive, and arousal hindbrain networks, demonstrating a genetic, developmental, and functional link between these diverse sensory systems.

Materials and Methods

Generation of an Inducible *Math1^{Cre*PR}* Line. We used a second-generation Cre-progesterone receptor fusion (*Cre*PR*), amplifying the sequence from pNN-hCre19V336A-PR650–914 (43). We ligated the *Cre*PR* with *Math1* 5′ and 3′ targeting arms such that the *Math1* transcription start site and first five *Math1* codons were preserved (5′ SphI and 3′ SalI insertion sites). To activate Cre*PR, 200 μg of RU486 (Mifepristone, Sigma) was administered to pregnant dams by interperitoneal injection at E9.5, E10.5, E11.5, E12.5, E13.5, E14.5, or E18.5. To prevent abortion, progesterone (Sigma) was coadministered (see *SI Text*).

Mouse Strains, Staging, and Genotyping. We used two *Math1*-null alleles which contain either *LacZ* (*Math1*^{LacZ}) or *HPRT* (*Math1*$^{-}$) in place of the *Math1* coding region (1, 2). The null embryos carried one *Math1*^{Cre*PR} allele and one *Math1*$^{-}$ allele. Three Cre reporter lines were used: *ROSA*^{LacZ}, *ROSA*^{EYFP}, and *Tau*$^{mGFP\_nLacZ}$ (19, 20, 29) (see *SI Text*).

Immunohistochemistry and X-gal Staining. E18.5/P0 brains were fixed 5–10 h in 4% PFA at 4° C and frozen sections were cut at 25 μm for soma analysis or 50 μm for projection analysis. Primary and secondary antibody staining, as well as X-gal staining, were performed as described (3, 6). Antibodies and their dilutions can be found online in the *SI Text*.

RNA in Situ Hybridization (ISH) Screen. The 24 probes were amplified from reverse-transcribed cDNA collected from P0 C57/B6 brainstem and cerebellum by using primers from the Allen Brain Atlas (www.brain-map.org). From 34 E18.5 hindbrains (18 WT, 16 null), coronal (3 sets each) and sagittal (15 sets each) 25-μm serial fresh frozen sections were cut. ISH for each probe was performed on complete sets from multiple littermate-matched WT and *Math1*-null hindbrains by using a robotic platform (44). Digital series were created from sections imaged at 1.2 μm/pixel [see Movies S1–S48 (AVI) and *SI Text* for list of probes). Image brightness and contrast were normalized by using Adobe Photoshop.

ACKNOWLEDGMENTS. We thank R. Atkinson, A. Liang, B. Antalffy, N. Ao, and Y. Liu for technical assistance, J. Dodd (Columbia University, New York, NY) for kindly providing the Lhx2/9 antibody, and T. Klisch, A. Flora, and B. Jusiak for comments on the manuscript. This work was supported by Gene Expression and Microscopy Cores Grant HD024064 of the Baylor Intellectual and Developmental Disabilities Research Center; M. F. R. was supported by National Research Service Award 5-F31-NS051046–03 from the National Institute of Neurological Disorders and Stroke and a Baylor Research Advocates for Student Scientists Scholarship; K. A. A. was supported by Pediatric Scientist Development Program Award K12-HD000850 from the National Institute of Child Health and Human Development. H. Y. Z. is an investigator of the Howard Hughes Medical Institute.

1. Ben-Arie N, et al. (2000) Functional conservation of atonal and Math1 in the CNS and PNS. *Development* 127:1039–1048.
2. Ben-Arie N, et al. (1997) Math1 is essential for genesis of cerebellar granule neurons. *Nature* 390:169–172.
3. Wang VY, Rose MF, Zoghbi HY (2005) Math1 expression redefines the rhombic lip derivatives and reveals novel lineages within the brainstem and cerebellum. *Neuron* 48:31–43.
4. Machold R, Fishell G (2005) Math1 is expressed in temporally discrete pools of cerebellar rhombic-lip neural progenitors. *Neuron* 48:17–24.
5. Englund C, et al. (2006) Unipolar brush cells of the cerebellum are produced in the rhombic lip and migrate through developing white matter. *J Neurosci* 26:9184–9195.
6. Bermingham NA et al. (2001) Proprioceptor pathway development is dependent on Math1. *Neuron* 30:411–422.
7. Akazawa C, Ishibashi M, Shimizu C, Nakanishi S, Kageyama R (1995) A mammalian helix-loop-helix factor structurally related to the product of Drosophila proneural gene atonal is a positive transcriptional regulator expressed in the developing nervous system. *J Biol Chem* 270:8730–8738.
8. His W (1891) Die entwicklung des menschlichen rautenhirns vom ende des ersten bis zum beginn des dritten monats. I. Verlangertes Mark. *Abhandlungen der koniglicher sachsischen Gesellschaft der Wissenschaften, Mathematische-physikalische Klasse* 29:1–74.
9. Altman J, Bayer SA (1997) *Development of the Cerebellar System: In Relation to its Evolution, Structure, and Functions* (CRC Press, Boca Raton, Florida).
10. Clarke A (1858) Researches on the intimate structure of the brain, human and comparative. First Series. On the structure of the medulla oblongata. *Philos Trans R Soc London* 148:231–259.
11. Wang TJ, Lue JH, Shieh JY, Wen CY (2000) Somatostatin-IR neurons are a major subpopulation of the cuneothalamic neurons in the rat cuneate nucleus. *Neurosci Res* 38:199–207.
12. Fredrich M, Reisch A, Illing RB (2009) Neuronal subtype identity in the rat auditory brainstem as defined by molecular profile and axonal projection. *Exp Brain Res* 195:241–260.
13. Cant NB, Benson CG (2003) Parallel auditory pathways: Projection patterns of the different neuronal populations in the dorsal and ventral cochlear nuclei. *Brain Res Bull* 60:457–474.
14. Cajal SRy (1909) *Histologie du Systeme Nerveux de l'Homme et des Vertebres* (Instituto Ramon y Cajal, Madrid); reprinted 1972, pp 774–838.
15. Held H (1893) Die centrale Gehorleitung. *Arch f Anat u Physiol Anat Ab* :201–248.
16. Fujiyama T, et al. (2009) Inhibitory and excitatory subtypes of cochlear nucleus neurons are defined by distinct bHLH transcription factors, Ptf1a and Atoh1. *Development* 136:2049–2058.
17. Altman J, Bayer SA (1987c) Development of the precerebellar nuclei in the rat: III. The posterior precerebellar extramural migratory stream and the lateral reticular and external cuneate nuclei. *J Comp Neurol* 257:513–528.
18. Taber–Pierce E (1973) Time of origin of neurons in the brain stem of the mouse. *Prog Brain Res* 40:53–65.
19. Soriano P (1999) Generalized lacZ expression with the ROSA26 Cre reporter strain. *Nat Genet* 21:70–71.
20. Srinivas S, et al. (2001) Cre reporter strains produced by targeted insertion of EYFP and ECFP into the ROSA26 locus. *BMC Dev Biol* 1:4.
21. Chizhikov VV, et al. (2006) The roof plate regulates cerebellar cell-type specification and proliferation. *Development* 133:2793–2804.
22. Miesegaes GR, et al. (2009) Identification and subclassification of new Atoh1 derived cell populations during mouse spinal cord development. *Dev Biol* 327:339–351.
23. Rose MF, et al. (2009) *Math1* is essential for the development of hindbrain neurons critical for perinatal breathing. *Neuron* 12:341–354.
24. Helms AW, Abney AL, Ben–Arie N, Zoghbi HY, Johnson JE (2000) Autoregulation and multiple enhancers control Math1 expression in the developing nervous system. *Development* 127:1185–1196.
25. Landsberg RL, et al. (2005) Hindbrain rhombic lip is comprised of discrete progenitor cell populations allocated by Pax6. *Neuron* 48:933–947.
26. Saba R, Johnson JE, Saito T (2005) Commissural neuron identity is specified by a homeodomain protein, Mbh1, that is directly downstream of Math1. *Development* 132:2147–2155.
27. Cheng L, et al. (2004) Tlx3 and Tlx1 are post-mitotic selector genes determining glutamatergic over GABAergic cell fates. *Nat Neurosci* 7:510–517.
28. Ugrumov MV, Melnikova VI, Lavrentyeva AV, Kudrin VS, Rayevsky KS (2004) Dopamine synthesis by non-dopaminergic neurons expressing individual complementary enzymes of the dopamine synthetic pathway in the arcuate nucleus of fetal rats. *Neuroscience* 124:629–635.
29. Hippenmeyer S, et al. (2005) A developmental switch in the response of DRG neurons to ETS transcription factor signaling. *PLoS Biol* 3:e159.
30. Gray PA (2008) Transcription factors and the genetic organization of brain stem respiratory neurons. *J Appl Physiol* 104:1513–1521.
31. Hirsch MR, Tiveron MC, Guillemot F, Brunet JF, Goridis C (1998) Control of noradrenergic differentiation and Phox2a expression by MASH1 in the central and peripheral nervous system. *Development* 125:599–608.
32. Hoshino M, et al. (2005) Ptf1a, a bHLH transcriptional gene, defines GABAergic neuronal fates in cerebellum. *Neuron* 47:201–213.
33. Sherrington CS (1906) *The Integrative Action of the Nervous System* (Yale Univ Press, New Haven, CT).
34. Altman J, Bayer SA (1980a) Development of the brain stem in the rat. I. Thymidine-radiographic study of the time of origin of neurons of the lower medulla. *J Comp Neurol* 194:1–35.
35. Vincent SR, Satoh K, Armstrong DM, Fibiger HC (1983) NADPH-diaphorase: A selective histochemical marker for the cholinergic neurons of the pontine reticular formation. *Neurosci Lett* 43:31–36.
36. Cummings S, Elde R, Ells J, Lindall A (1983) Corticotropin-releasing factor immunoreactivity is widely distributed within the central nervous system of the rat: An immunohistochemical study. *J Neurosci* 3:1355–1368.
37. Barrington F (1925) The effect of lesions of the hind- and mid-brain on micturition in the cat. *Q J Exp Physiol* 15:81–102.
38. Rouzade–Dominguez ML, Pernar L, Beck S, Valentino RJ (2003) Convergent responses of Barrington's nucleus neurons to pelvic visceral stimuli in the rat: A juxtacellular labelling study. *Eur J Neurosci* 18:3325–3334.
39. Valentino RJ, Chen S, Zhu Y, Aston–Jones G (1996) Evidence for divergent projections to the brain noradrenergic system and the spinal parasympathetic system from Barrington's nucleus. *Brain Res* 732:1–15.
40. Leonard CS, Kerman I, Blaha G, Taveras E, Taylor B (1995) Interdigitation of nitric oxide synthase-, tyrosine hydroxylase-, and serotonin-containing neurons in and around the laterodorsal and pedunculopontine tegmental nuclei of the guinea pig. *J Comp Neurol* 362:411–432.
41. Reese NB, Garcia–Rill E, Skinner RD (1995) The pedunculopontine nucleus–auditory input, arousal and pathophysiology. *Prog Neurobiol* 47:105–133.
42. Timofeeva E, Dufresne C, Sik A, Zhang ZW, Deschenes M (2005) Cholinergic modulation of vibrissal receptive fields in trigeminal nuclei. *J Neurosci* 25:9135–9143.
43. Wunderlich FT, Wildner H, Rajewsky K, Edenhofer F (2001) New variants of inducible Cre recombinase: a novel mutant of Cre-PR fusion protein exhibits enhanced sensitivity and an expanded range of inducibility. *Nucleic Acids Res* 29:E47.
44. Yaylaoglu MB, et al. (2005) Comprehensive expression atlas of fibroblast growth factors and their receptors generated by a novel robotic in situ hybridization platform. *Dev Dyn* 234:371–386.